

## Tổng hợp xanh vật liệu khung kim loại-hữu cơ $Cu_3BTC_2$ loại bỏ methylene blue trong môi trường nước

Nguyễn Thị Thu Hương<sup>1</sup>, Nguyễn Văn Bằng<sup>2</sup>, Nguyễn Thị Lan Anh<sup>2</sup>,  
Trịnh Dương Vương<sup>3</sup>, Nguyễn Mạnh Tiến<sup>4</sup>, Đỗ Bình Minh<sup>1</sup>,  
Lã Đức Dương<sup>2</sup>, Nguyễn Thị Hoài Phương<sup>2,\*</sup>

<sup>1</sup>Viện Công nghệ mới, Viện Hàn lâm Khoa học và Công nghệ Việt Nam, Việt Nam

<sup>2</sup>Phân viện Hóa-Môi trường, Trung tâm Nhiệt đới Việt-Nga, Việt Nam

<sup>3</sup>Trường Sĩ quan Không quân, Việt Nam

<sup>4</sup>Viện Kỹ thuật Phòng không - Không quân, Việt Nam

Ngày nhận bài: 10/09/2023; Ngày sửa bài: 14/12/2023;

Ngày nhận đăng: 17/01/2024; Ngày xuất bản: 28/02/2024

### TÓM TẮT

Nghiên cứu này trình bày kết quả nghiên cứu tổng hợp, mô tả đặc trưng và khả năng hấp phụ của vật liệu khung cơ kim trên cơ sở Cu(II) và phối tử hữu cơ 1,3,5-benzene tricarboxylate (Cu-BTC). Cu-BTC được tổng hợp bằng phương pháp vi sóng đơn giản và được đo FTIR, SEM, XRD để kiểm tra đặc tính liên kết, hình thái, cấu trúc tinh thể. Cu-BTC được sử dụng làm chất hấp phụ để loại bỏ thuốc nhuộm họ azo như methylene blue (MB) trong nước. Các nghiên cứu về ảnh hưởng của pH, nồng độ, thời gian hấp phụ cho thấy loại bỏ MB theo mô hình hấp phụ đẳng nhiệt Freundlich và mô hình động học biểu kiến bậc hai. Do đó, cơ chế hấp phụ MB đa lớp trên bề mặt Cu-BTC không đồng nhất và chịu ảnh hưởng của lực hút tĩnh điện. Những đặc trưng này cho thấy Cu-BTC là vật liệu hứa hẹn trong việc loại bỏ MB ra khỏi nước thải định hướng ứng dụng tiềm năng trong xử lý môi trường.

**Keywords:** Hóa học xanh, vật liệu khung kim loại-hữu cơ, kỹ thuật vi sóng, methylene blue, xử lý môi trường.

\*Tác giả liên hệ chính.

Email: hoaiphuong1978@gmail.com

# Green synthesis of metal-organic framework material $\text{Cu}_3\text{BTC}_2$ removes methylene blue from aqueous media

Thu Huong Nguyen Thi<sup>1</sup>, Van Bang Nguyen<sup>2</sup>, Lan Anh Nguyen Thi<sup>2</sup>,  
Duong Vuong Trinh<sup>3</sup>, Manh Tien Nguyen<sup>4</sup>, Binh Minh Do<sup>1</sup>,  
Duc Duong La<sup>2</sup>, Hoai Phuong Nguyen Thi<sup>2,\*</sup>

<sup>1</sup>*Institute of New Technology, Vietnam Academy of Science and Technology, Vietnam*

<sup>2</sup>*Department of Chemistry and Environment, Joint Vietnam-Russia Tropical Science  
and Technology Research Center, Vietnam*

<sup>3</sup>*Air Force Officer School, Vietnam*

<sup>4</sup>*Institute of Technology Air Defense - Air Force, Vietnam*

*Received: 10/09/2023; Revised: 14/12/2023;*

*Accepted: 17/01/2024; Published: 28/02/2024*

## ABSTRACT

This study presents the results of the synthesis, characterization, and adsorption capacity of organometallic framework materials based on Cu(II) and the organic ligand 1,3,5-benzene tricarboxylate (Cu-BTC). Cu-BTC was synthesized by simple microwave method, and FTIR, SEM, and XRD were measured to check the bonding, morphology, and crystal structure properties. Cu-BTC is an adsorbent to remove azo dyes such as methylene blue (MB) from water. Studies on the effects of pH, concentration, and adsorption time showed that MB was removed according to the Freundlich isotherm adsorption model and the apparent second-order kinetic model. Therefore, the multilayer MB adsorption mechanism on the Cu-BTC surface is heterogeneous and influenced by electrostatic attraction. These characteristics show that Cu-BTC is a promising material for removing MB from wastewater with potential applications in environmental treatment.

**Từ khóa:** *Green chemistry, metal-organic frameworks, microwave method, methylene blue, environment treatment.*

## 1. INTRODUCTION

Textile industry wastewater has severe impacts on living organisms. It must be treated to a certain extent before being released into the environment. Dyeing process wastewater contains non-biodegradable and high-toxic pigments,<sup>1</sup> which have been found to damage the balance<sup>2-4</sup> and integrity of ecological systems<sup>5,6</sup> and have carcinogenic effects on long-term exposure.<sup>7-9</sup> Therefore, wastewater treatment in

the textile dyeing industry has become a concern on a global scale.<sup>10,11</sup> In this context, researchers have proposed metal-organic frameworks (MOFs) as one of the effective methods to remove dye wastewater.<sup>12-14</sup> MOF exhibits high adsorption capacity in dye removal with tunable pore diameter and surface morphology compared with other conventional adsorbent materials such as activated carbon,<sup>15,16</sup> carbon nanotubes,<sup>17</sup> zeolites,<sup>18</sup> etc. In addition, the metal-organic

---

\*Corresponding author.

Email: [hoaihuong1978@gmail.com](mailto:hoaihuong1978@gmail.com)

framework material also has a significant photocatalytic activity for treating different dye types.<sup>19-21</sup> These studies also evaluated the effectiveness of these MOFs in the process of dye removal from wastewater. Metal-organic frameworks based on copper (II) have also been synthesized, modified, combined, doped, hybridized... and evaluated for their ability to remove dyes in water environments.<sup>22,23</sup>

Many studies have applied different synthesis methods to fabricate copper-based metal-organic frameworks. Solvothermal, one-step in situ growth, and pre-grinding methods have all been studied to synthesize this material.<sup>24,25</sup> Synthesis of MOFs has also been of interest to meet green chemistry requirements where selection of synthesis elements has been based on reduced energy input, safe reaction solvents (such as water and supercritical solvents), continuous manufacturing method, and performance design of MOFs through theoretical predictions.<sup>26,27</sup> In this study, copper-based metal-organic framework (Cu-BTC) was synthesized green by microwave method using water/ethanol mixed solvent mixture. Cu-BTC was also evaluated for its ability to remove dyes in water through pure adsorption and simultaneous catalytic-adsorption mechanisms.

## 2. EXPERIMENTAL

### 2.1. Chemicals, equipment and tools

Copper (II) chloride dihydrate ( $\text{CuCl}_2 \cdot 2\text{H}_2\text{O}$  99%) was purchased from Xilong Chemical Co., Ltd., Guangdong, China. 1,3,5-benzene tricarboxylic acid ( $\text{H}_3\text{BTC}$  98%) is imported from Shanghai Macklin Biochemical Co., Ltd., Shanghai, China. Methylene blue ( $\text{C}_{16}\text{H}_{18}\text{ClN}_3\text{S}$ , MB  $\geq$  85%) was gotten from Merck, Germany. Ethanol solution ( $\text{C}_2\text{H}_5\text{OH}$  96%), Sodium hydroxide ( $\text{NaOH}$  > 96%), and Hydrochloric acid ( $\text{HCl}$  > 35%) were bought from Duc Giang Chemical, Vietnam. Double distilled water is made in the laboratory.

The equipment used in the experiment includes an Electrolux microwave oven (50 Hz,

1050 W), drying cabinet, and Ultrasonic Cleaner Ultrasonic Cleaner JP-060S made in China; Centrifuge Hettich Universal 320 from Germany.

### 2.2. Material synthesis

The material was synthesized from  $\text{CuCl}_2$ : Weigh 1.7 g of  $\text{CuCl}_2 \cdot 2\text{H}_2\text{O}$  into a 250 mL beaker, then add 100 mL distilled water, add 2.8 g  $\text{H}_3\text{BTC}$  acid, and stir well. Put the glass cup in the microwave (reaction conditions are 45 min, 80 °C). Next, filter and wash the precipitate with ethanol and distilled water 5 times using an ultrasonic cleaner, and then centrifuge at 7,000 rpm for 10 min with a centrifuge to obtain a very blue solid product. Then, the solid product is dried at 120 °C for 2 hours in a drying oven. Store the synthetic material in a tightly closed plastic container and use it for the following experiments.

### 2.3. Techniques and methods

*Characterizations.* The functional groups present in the material were determined using the FTIR infrared spectroscopy technique in the 400–4000  $\text{cm}^{-1}$  wavelength range. The material's morphology was observed using scanning electron microscopy techniques with magnification capabilities up to 100,000 times. The crystal structure of the Cu-BTC framework material in powder form was analyzed through an X-ray diffraction analyzer-D8-Advance. At 1.54 Å in a copper X-ray tube ( $\text{Cu-K}\alpha$ ), the device is operated at 44 mA and 40 kV voltage. The scanning speed is 0.2 °/min to measure materials in the range ( $2\theta$ ) from 10° to 70°.

*Methylene blue adsorption.* The MB solution (1 g/L) was diluted with distilled water twice to prepare the required MB solution concentrations (10, 20, 30, 40, and 50 mg/L). Methylene blue (MB) was used as a dye to study the adsorption capacity of the synthesized Cu-BTC organometallic framework. The pH of the MB solution was normalized with 1 M NaOH solution and 1 M HCl solution. Conducting experiments on the influence of pH on the MB adsorption process. 10 mg of Cu-BTC

was added to each test tube containing 20 mL of MB solution. Each glass test tube with MB solution pH of 3, 5, 7, 9, and 11, respectively, was sealed with a rubber stopper, put into a closed light-blocking cabinet, and a light cabinet to study the effect of light. Then, the test tubes were thoroughly mixed by ultrasonic washing for 15 minutes, shaking with a shaker at 200 rpm at room temperature to filter the solution, and finally, photometrically. UV-Vis spectrum at maximum absorption wavelength to determine MB concentration based on the linear equation from the MB standard curve. Experiments to investigate the effect of pH on dye handling were carried out under the same conditions. Sample dilution was performed with double distilled water if the MB solution concentration value exceeded the maximum adsorption limit of the graph containing the MB calibration curve. Investigation of the kinetics of the adsorption process by influencing factors of pH, adsorption time, and initial MB solution concentration with the same amount of Cu-BTC adsorbent at equilibrium time was studied the same as above. The maximum wavelength of the MB solution is determined to be 662 nm. The equation can determine the concentration of MB solution at time t (unit is mg/L) to be

$C = (Abs - 0.0216)/0.1587$  ( $R^2 = 0.9985$ ), where A is the light absorption intensity.

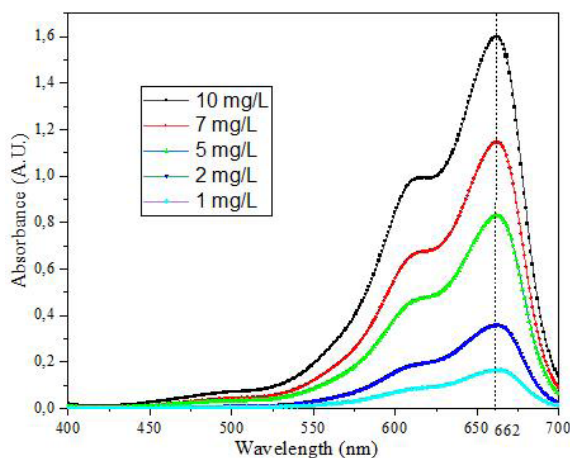


**Figure 1.** UV-Vis spectra of the MB standard sample at 400 to 700 nm wavelengths.

The MB removal efficiency of the material is calculated according to the equation:

$$H = \frac{C_0 - C_t}{C_0} \times 100\%$$

The adsorption capacity was calculated according to the formula:

$$q_t = \frac{V \times (C_0 - C_t)}{m}$$

Where  $C_0$  and  $C_t$  are the initial concentration of MB solution and at time t (mg/L), respectively; V is the volume of MB solution used (L), and m is the mass of Cu-BTC (g).

*Isothermal and kinetics of MB adsorption.*

Langmuir, Freundlich, and Temkin adsorption models are used to describe the adsorption equilibrium as follows:

Langmuir model:  $\frac{C_e}{q_e} = \frac{1}{K_L q_m} + \frac{C_e}{q_m}$

Freundlich model:  $\ln q_e = \ln K_F + \frac{1}{n} \ln C_e$

Temkin model:  $q_e = B_T \ln K_T + B_T \ln C_e$

$$B_T = \frac{RT}{b_T}$$

In which  $q_e$  is the equilibrium adsorption capacity (mg/g),  $q_m$  is the maximum adsorption capacity (mg/g),  $K_L$  is the Langmuir constant (L/mg),  $K_F$  is the Freundlich [(mg/g)(L/mg)<sup>1/n</sup>], and  $K_T$  is the Temkin constant (L/g);  $C_e$  is the equilibrium concentration of adsorbent (mg/L); n is Freundlich's linear constant,  $b_T$  is related to the adsorption heat, R is the universal gas constant and T is the temperature. The Langmuir adsorption model assumes that all adsorption sites have the same affinity and reach a maximum value for the adsorbent and adsorbate after forming a monolayer on a uniform adsorbent surface at a specific temperature and no interactions between the adsorbed molecules. In contrast to the Langmuir model, the Freundlich model assumes that the adsorption surface energy is heterogeneous. The n value represents

the deviation from the linearity, the heterogeneity of the adsorption site. If  $n$  is between 1 and 10, then the adsorption is favorable. The larger  $n$  is, the higher the heterogeneity of the adsorption site. The Temkin is a chemical adsorption model based on the interaction between positive and negative charges.

To elucidate the adsorption kinetic process of MB on Cu-BTC, three apparent kinetic models, namely first-order, second-order, and intra-particle diffusion, are considered to explain the experimental data:

First-order apparent kinetic model:

$$\ln(q_e - q_t) = \ln(q_e) - k_1 t$$

Second-order apparent kinetic model:

$$\frac{t}{q_t} = \frac{1}{k_2 q_e^2} + \frac{t}{q_e}$$

Particle diffusion model:  $q_t = k_1 t^{1/2} + C$

In which  $q_e$ ,  $q_t$  is the adsorption capacity at equilibrium time and at time  $t$  on the material (mg/g), respectively;  $k_1$  is the first-order apparent adsorption rate constant ( $\text{min}^{-1}$ ),  $k_2$  is the second-order apparent adsorption rate constant ( $\text{g}/\text{mg}\cdot\text{min}$ );  $C$  is the blocking coefficient in the particle and  $k_1$  is the diffusion rate constant in the particle ( $\text{mg}/\text{g}\cdot\text{min}^{1/2}$ ).

### 3. RESULTS AND DISCUSSION

#### 3.1. Characterization

The FTIR spectra of the  $\text{H}_3\text{BTC}$  sample and the Cu-BTC organometallic framework material (Figure 2) contain characteristic peaks at  $\sim 1640$ ,  $\sim 1447$ , and  $\sim 1370 \text{ cm}^{-1}$ . FTIR spectrum of Cu-BTC using KBr in the  $400\text{-}1700 \text{ cm}^{-1}$  range. The peaks at  $\sim 1640$ ,  $\sim 1447$ , and  $\sim 1370 \text{ cm}^{-1}$  characteristically bond the carboxylate group  $-\text{COO}-$  in Cu-BTC, indicating the formation of Cu-BTC organometallic framework material.<sup>28,29</sup> The broad bands at  $3346 \text{ cm}^{-1}$  are believed to be OH bonds and water adsorbed on the Cu-BTC surface. In addition, no peak was observed in the  $1680\text{-}1750 \text{ cm}^{-1}$  range, which shows no

free  $\text{H}_3\text{BTC}$  ligand in the Cu-BTC material.<sup>28</sup> The range  $1500\text{-}1400 \text{ cm}^{-1}$  represents the  $\text{C}=\text{C}$  bond in the aromatic ring.<sup>28</sup> The FTIR shows the carbonyl group in  $\text{H}_3\text{BTC}$  peaks at  $1721 \text{ cm}^{-1}$ .<sup>29</sup> The  $-\text{CO}-\text{C}$  bond in Cu-BTC is demonstrated by the appearance of the peak at about  $1109 \text{ cm}^{-1}$ . The  $827\text{-}1153 \text{ cm}^{-1}$  range belonged to the  $\text{OC}=\text{O}$  and  $\text{CO}$  bond of 1,4 benzene dicarboxylic acid. At  $487 \text{ cm}^{-1}$  and  $728 \text{ cm}^{-1}$ , it is assigned the CH bond of the benzene ring and the Cu-O bond form between the carboxylic groups of  $\text{H}_3\text{BTC}$  and Cu(II), respectively.<sup>30,31</sup>

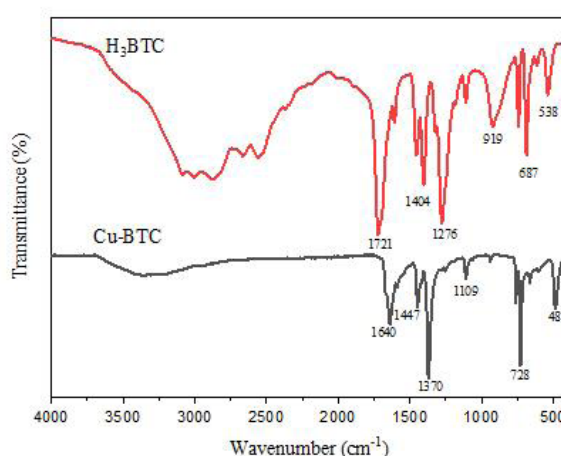


Figure 2. FTIR spectrum of  $\text{H}_3\text{BTC}$  and Cu-BTC.

SEM image of Cu-BTC material in Figure 3. Cu-BTC crystal particles have an octahedral shape. Cu-BTC morphology is consistent with other reported SEM images.<sup>28,32,33</sup> Some particles that do not have a characteristic morphology in the SEM images are fused particles of Cu-BTC crystals.

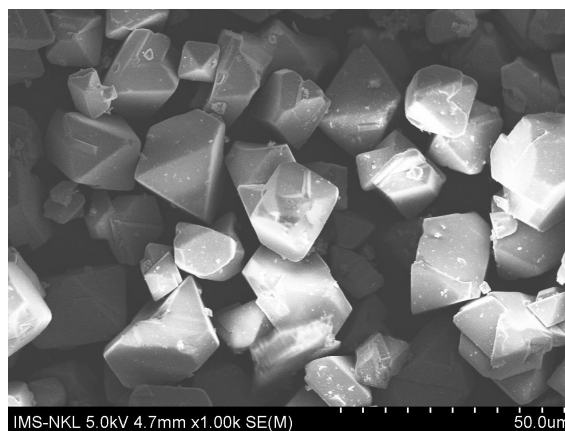
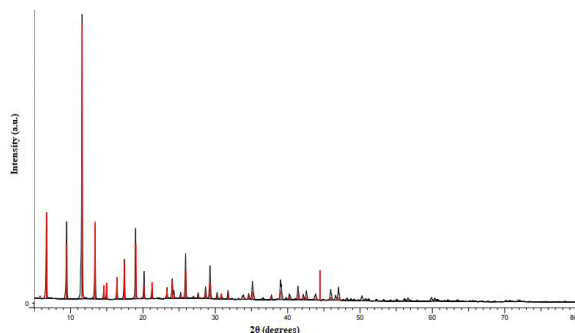


Figure 3. SEM images of Cu-BTC.



**Figure 4.** XRD patterns of Cu-BTC.

X-ray diffraction (XRD) analysis examined the crystal structure of the powdered Cu-BTC in Figure 4. The characteristic peaks are found in the Cu-BTC crystalline in the range up to  $2\theta$ , namely  $11.6^\circ$ ,  $13.5^\circ$ ,  $14.9^\circ$ , and  $16.6^\circ$  corresponding to the crystal faces (222), (400), (420), (422) and is consistent with the published study,<sup>28,32,34-37</sup> which shows that metal-organic frameworks are successfully fabricated. The peak with the highest intensity at  $2\theta = 11.59^\circ$  is related to the high degree of crystallinity of the material.<sup>30</sup> XRD and SEM spectrum results show the successful fabrication of Cu-BTC.

### 3.2. Effect of pH on the adsorption of methylene blue

The adsorption capacity of the MB solution is significantly influenced by its pH level.<sup>38</sup> Figure 5 and Table 1 show that the optimal pH for methylene blue adsorption onto Cu-BTC is  $\text{pH} \sim 7$ . The results are similar to previous studies.<sup>30-39</sup>

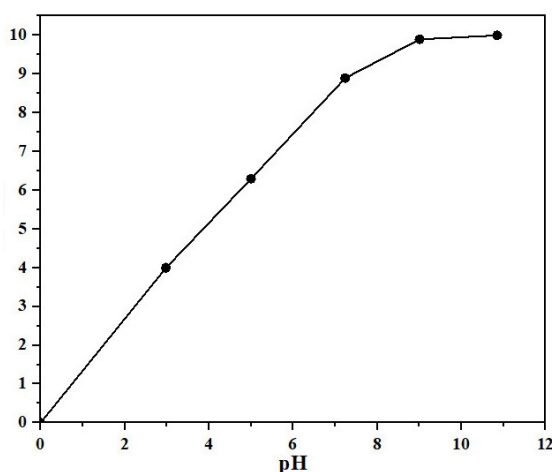


**Figure 5.** Effect of pH on the adsorption capacity of MB. Experimental conditions include  $25^\circ\text{C}$ , 0.011 g Cu-BTC.

The adsorption capacity of MB increases when the pH rises from 4 to 7. However, the adsorption capacity remained almost constant with an increase in pH from 7 to 11. The point of zero charge of pH ( $\text{pH}_{\text{PZC}}$ ) for Cu-BTC material was found to be 4.<sup>40</sup> When  $\text{pH} < 4$ , the surface of the adsorbent turns positively charged, and the adsorption process of methylene blue onto Cu-BTC is difficult. When  $\text{pH} \geq 4$ , the surface of the adsorbent turns negatively charged, and this process is easy. When  $4 \leq \text{pH} < 7$ ,  $\text{H}^+$  ions compete with dye cations through electrostatic attraction, causing a decrease in adsorption. It is possible that a low pH might not be suitable for adsorption of MB. When pH increases, the MB solution containing  $\text{Cl}^-$  binds to Cu-BTC material quickly and reacts with NaOH to form NaCl and MB-S+ OH. The mass of NaCl can change the adsorption of MB-S+ OH on the surface of Cu-BTC material. While  $\text{pH} \sim 7$ , the hydrolysis process to release MB molecules is negligible.

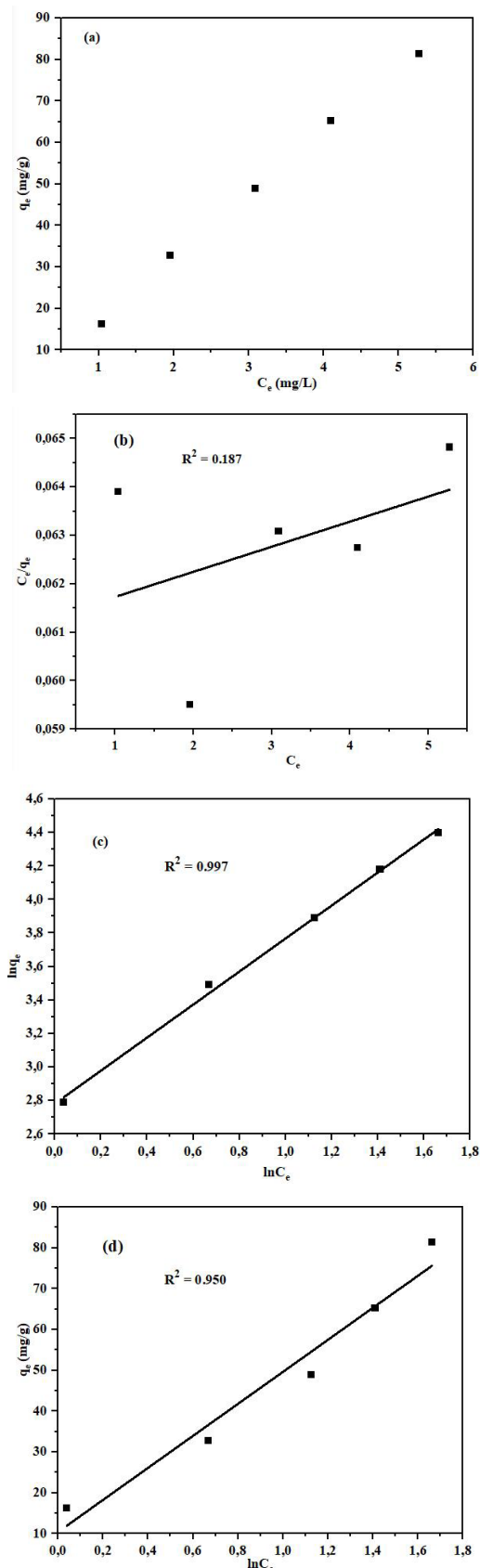
**Table 1.** Effect of pH on removal of MB after 30 minutes of Cu-BTC in adsorption processes.

pH	$C_t$ (mg/L)	H (%)	$q_t$ (mg/g)
2.98	7.83	21.7	4.0
5.00	6.56	34.4	6.3
7.24	5.11	48.9	8.9
9.01	4.54	54.6	9.9
10.85	4.48	55.2	10.0

Note: Experimental conditions include  $25^\circ\text{C}$ , 0.011 g Cu-BTC, and 20 mL of 10 mg/L MB solution.

### 3.3. Isothermal and Kinetics of MB adsorption

The ability and mechanism of MB dye adsorption of Cu-BTC were investigated and predicted through adsorption experiments. The isotherm of the adsorption process explains the reaction mechanism between MB molecules and Cu-BTC, helping to optimize the factors affecting the adsorption process. Kinetic models were studied to better explain the reaction mechanism by analyzing adsorption capacity over time.



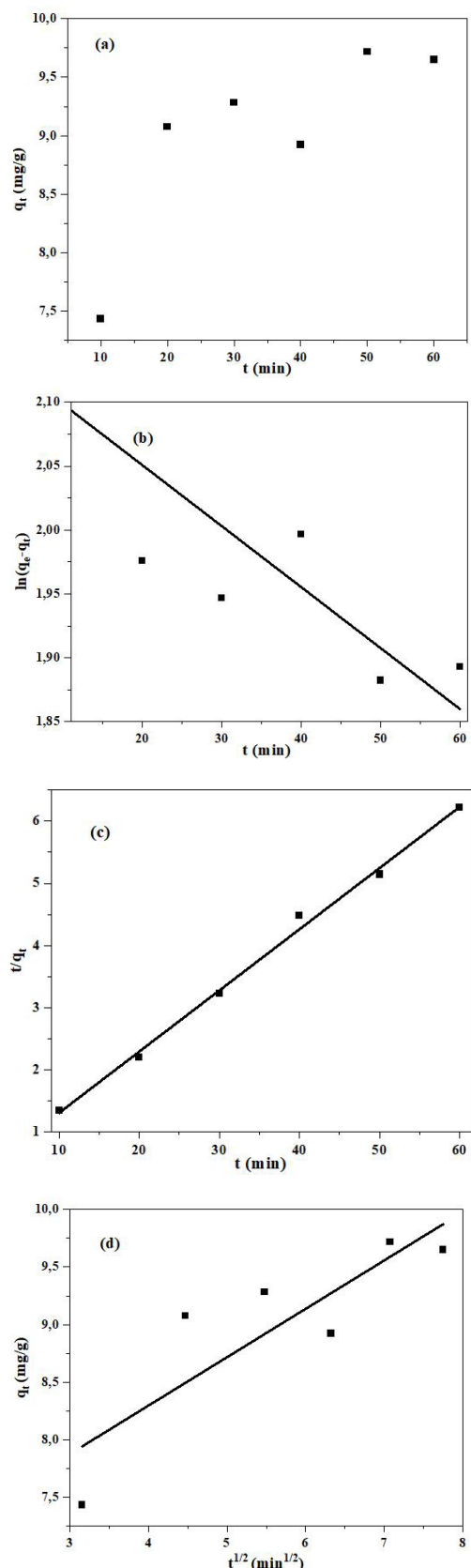
**Figure 6.** The adsorption isotherm of MB on Cu-BTC (a), (b) Langmuir adsorption model, (c) Freundlich adsorption model, (d) Temkin adsorption model.

Figure 6 shows the isotherm modeling results of MB onto Cu-BTC, and the model parameters of the three isotherms are summarized in Table 2. The Freundlich isotherm model fits the concentration quite well. Test (correlation coefficient  $R^2 = 0.9968$ ). The Temkin model ( $R^2 = 0.9503$ ) fits reasonably well. The value  $n = 1.01$  for the Freundlich isotherm model demonstrates the suitability of this model with experimental data. The results show the adsorption mechanism on heterogeneous surfaces, heterogeneous surfaces, and multilayer adsorption, which is also consistent with the characteristics of the synthesized materials. However, the maximum adsorption capacity of the material calculated according to the Langmuir model reached 1929.5 mg/g, higher than the absorption capacity of other materials, such as nano  $Fe_3O_4$  (161.8 mg/g), tannic acid/graphene nanocomposite (200 mg/g).<sup>28</sup> Due to its high adsorption capacity and simple synthesis process, Cu-BTC is considered one of the essential materials for MB removal.

**Table 2.** Parameter values of Langmuir, Freundlich, and Temkin adsorption isotherm equations of MB on Cu-BTC.

Isotherms	Parameters	Value
<b>Langmuir</b>	$q_m$ (mg/g)	1,929.5
	$K_L$ (L/mg)	0.0085
	$R^2$	0.187
<b>Freundlich</b>	$K_F [(mg/g)(L/mg)^{1/n}]$	16.139
	$n$	1.01
	$R^2$	0.997
<b>Temkin</b>	$K_T$ (L/g)	1.30
	$b_T$ (J/mol)	63.15
	$R^2$	0.950

Initial concentration and adsorption time are essential parameters for the adsorption capacity of MB on Cu-BTC. As shown in Table 3, at the same initial concentration, the adsorption capacity of MB on the Cu-BTC organometallic



**Figure 7.** Effect of time on adsorption capacity (a), model of apparent first-order (b), apparent second-order (c), intra-particle diffusion (d) for MB adsorption on Cu-BTC.

framework material increased as the adsorption time increased. Similarly, in Figure 7a, at five different initial concentrations of MB of 10, 20, 30, 40, and 50 mg/L, the adsorption capacity of MB on the Cu-BTC organometallic framework material increased when The initial concentration of MB increased. That shows that the adsorption efficiency depends on the adsorption time and initial concentration of MB.

**Table 3.** Effect of time on MB adsorption of Cu-BTC in the adsorption process.

Time (min)	C <sub>t</sub> (mg/L)	H (%)
10	5.91	40.9
20	5.01	49.9
30	4.89	51.1
40	5.09	49.1
50	4.65	53.5
60	4.69	53.1

Note: Experimental conditions are pH = 7.24; 25 °C, 0.011 g Cu-BTC; 20 mL of MB solution, initial concentration of MB is 10 mg/L.

The three models are shown in Figure 7, and their kinetic parameters are presented in Table 4.

Note: Experimental conditions are pH = 7.24; 25 °C, 0.011 g Cu-BTC; 20 mL of MB solution, the initial concentrations of MB are 10, 20, 30, 40, and 50 mg/L, respectively.

**Table 4.** Parameters of the apparent kinetic equation of MB adsorption onto Cu-BTC with an initial 10 mg/L concentration.

Kinetic model	Parameter	Value
First-order apparent model	k <sub>1</sub> (min <sup>-1</sup> )	-8.10 <sup>-5</sup>
	q <sub>e,cal</sub> (mg/g)	8.55
	q <sub>e,exp</sub> (mg/g)	16.29
	R <sup>2</sup>	0.5957
Second-order apparent model	k <sub>2</sub> (g/mg.min)	0.0296
	q <sub>e,cal</sub> (mg/g)	10.16
	q <sub>e,exp</sub> (mg/g)	16.29
	R <sup>2</sup>	0.9948
Intraparticle diffusion model	k <sub>i</sub> (mg/g.min <sup>1/2</sup> )	0.42075
	C (mg/g)	6.61
	R <sup>2</sup>	0.6692

From Table 4, it can be seen that the correlation coefficient  $R^2$  of the apparent quadratic model ( $R^2 = 0.9948$ ) is more significant than that of the clear first-order model ( $R^2 = 0.5957$ ), and the model experimental diffusion pattern ( $R^2 = 0.6692$ ). In addition, the equilibrium adsorption capacity value calculated according to the apparent quadratic kinetic equation ( $q_{e,cal}$ ) is much closer to the experimentally calculated adsorption capacity value ( $q_{e,exp}$ ) than the value. The adsorption capacity value was calculated according to the apparent first-order kinetic equation. These results indicate that the apparent first-order model does not describe the adsorption process. From that, the apparent second-order kinetic model describes the MB adsorption process for the entire adsorption time. However, the apparent first- and second-order models could not determine the diffusion mechanism of MB adsorption on Cu-BTC MOFs, so the intra-particle diffusion model was used to determine the diffusion mechanism. Table 4 shows that the correlation coefficient model  $R^2$  of the particle diffusion kinetics model ( $R^2 = 0.6692$ ) is lower than that of the apparent quadratic model. The adsorption process is related to the diffusion of particles. Dispersed in the particles, it is not the only factor affecting adsorption. Therefore, the adsorption process occurs in an apparent second-order pattern and is controlled by other factors such as pH.

#### 4. CONCLUSION

This study used a simple microwave method to synthesize Cu-BTC organometallic framework material to remove MB in water. The synthesized Cu-BTC MOFs have octahedral morphology. Studies on the effects of pH, concentration, and adsorption time showed that MB was removed according to the Freundlich isotherm adsorption model and the apparent second-order kinetic model. Therefore, the multilayer MB adsorption mechanism on the surface of Cu-BTC MOFs is not uniform and is influenced by electrostatic attraction. These characteristics show that Cu-BTC MOFs are ideal for further research on

MB removal from wastewater and potential applications in environmental research.

#### Acknowledgment

*This research is conducted and funded by the Department of Inorganic Materials, Institute of Chemistry and Materials.*

#### REFERENCES

1. V. Z. Sönmez, N. Sivri. Change of acute toxicity of dyestuff wastewaters, *Polish Journal of Environmental Studies*, **2020**, 29(1), 491-498.
2. P. O. Oladoye, T. O. Ajiboye, E. O. Omotola, O. Oyewola. Methylene blue dye: toxicity and potential technologies for elimination from (waste) water, *Results in Engineering*, **2022**, 16(6), 100678.
3. T. Tomar, N. Kahandawala, J. Kaur, L. Thounaojam, I. Choudhary, S. Bera. Bioremediation of synthetic dyes from wastewater by using microbial nanocomposites: an emerging field for water pollution management, *Biocatalysis and Agricultural Biotechnology*, **2023**, 51, 102767.
4. P. O. Oladoye, O. M. Bamigboye, O. D. Ogunbiyi, M. T. Akano. Toxicity and decontamination strategies of Congo red dye, *Groundwater for Sustainable Development*, **2022**, 19(1), 100844.
5. M. Andriamanantena, F. F. Razafimbelo, B. Raonizafinimanana, D. Cardon, P. Danthu, J. Lebeau, T. Petit, Y. Caro. Alternative sources of red dyes with high stability and antimicrobial properties: towards an ecological and sustainable approach for five plant species from Madagascar, *Journal of Cleaner Production*, **2021**, 303, 126979.
6. W. U. Khan, S. Ahmed, Y. Dhoble, S. Madhav. A critical review of hazardous waste generation from textile industries and associated ecological impacts, *Journal of the Indian Chemical Society*, **2023**, 100(1), 100829.
7. P. S. Preethi, S. Vickram, R. Das, N. M. Hariharan, M. Rameshpathy, R. Subbaiya, N. Karmegam, W. Kim, M. Govarthan. Bioprospecting of novel peroxidase from streptomyces coelicolor strain

- SPR7 for carcinogenic azo dyes decolorization, *Chemosphere*, **2023**, *310*, 136836.
8. S. A. Bhat, F. Zafar, A. U. Mirza, P. Singh, A. H. Mondal, N. Nishat. Nanovertegerie: bactericidal polymer nanocomposite beads for carcinogenic dye removal from aqueous solution, *Journal of Molecular Structure*, **2023**, *1284*, 135232.
  9. M. M. Haque, M. A. Haque, M. K. Mosharaf, A. Rahman, M. S. Islam, K. Nahar, A. H. Molla. Enhanced biofilm-mediated degradation of carcinogenic and mutagenic azo dye by novel bacteria isolated from tannery wastewater, *Journal of Environmental Chemical Engineering*, **2023**, *11*(5), 110731.
  10. S. Samsami, M. Mohamadizani, M. H. Sarrafzadeh, E. R. Rene, M. Firoozbahr. Recent advances in the treatment of dye-containing wastewater from textile industries: overview and perspectives, *Process Safety and Environmental Protection*, **2020**, *143*(10), 138-163.
  11. S. K. Selvi, M. Eswaramurthi. Treatment of textile dyeing wastewater using a low-cost adsorbent, *Materials Today: Proceedings*, **2023** (in press).
  12. S. Sağlam, F. N. Türk, H. Arslanoğlu. Use and applications of metal-organic frameworks (MOF) in dye adsorption, *Journal of Environmental Chemical Engineering*, **2023**, *11*(5), 110568.
  13. I. Salahshoori, M. N. Jorabchi, S. Ghasemi, M. Golriz, S. Wohlrab, H. A. Khonakdar. Advancements in wastewater treatment: a computational analysis of adsorption characteristics of cationic dyes pollutants on amide functionalized-MOF nanostructure MIL-53 (Al) surfaces, *Separation and Purification Technology*, **2023**, *319*, 124081.
  14. Y. Zhao, H. Zhou, M. Song, Z. Xu, Z. Sun, Q. Xu, Y. Chen, X. Liao. Interface engineering of Ti-MOFs: adsorption of anionic, cationic and neutral dyes in wastewater, *Journal of Molecular Structure*, **2023**, *1283*, 135268.
  15. A. Vakili, A. A. Zinatizadeh, Z. Rahimi, S. Zinadini, P. Mohammadi, S. Azizi, A. Karami, M. Abdulgader. The impact of activation temperature and time on the characteristics and performance of agricultural waste-based activated carbons for removing dye and residual COD from wastewater, *Journal of Cleaner Production*, **2023**, *382*, 134899.
  16. N. Kumar, A. Pandey, Rosy, Y. C. Sharma. A review on sustainable mesoporous activated carbon as adsorbent for efficient removal of hazardous dyes from industrial wastewater, *Journal of Water Process Engineering*, **2023**, *54*, 104054.
  17. D. D. Hu, Y. D. Li, Y. Weng, H. Q. Peng, J. B. Zeng. Mussel inspired stable underwater superoleophobic cotton fabric combined with carbon nanotubes for efficient oil/water separation and dye adsorption, *Applied Surface Science*, **2023**, *631*, 157566.
  18. M. Mahamud, A. M. Tadesse, Y. Bogale, Z. Bezu. Zeolite supported CdS/TiO<sub>2</sub>/CeO<sub>2</sub> composite: synthesis, characterization and photocatalytic activity for methylene blue dye degradation, *Materials Research Bulletin*, **2023**, *161*, 112176.
  19. X. Y. Lu, M. L. Zhang, Y. X. Ren, J. J. Wang, X. G. Yang. Design of Co-MOF nanosheets for efficient adsorption and photocatalytic degradation of organic dyes, *Journal of Molecular Structure*, **2023**, *1288*, 135796.
  20. D. Mukherjee, B. V. Bruggen, B. Mandal. Advancements in visible light responsive MOF composites for photocatalytic decontamination of textile wastewater: a review, *Chemosphere*, **2022**, *295*, 133835.
  21. V. Singh, S. Gautam, S. Kaur, N. Kajal, M. Kaur, R. Gupta. Highly functionalized photo-activated metal-organic frameworks for dye degradation: recent advancements, *Materials Today Communications*, **2023**, *34*, 105180.
  22. A. H. Shah, Z. U. Abideen, S. Maqsood, F. Rashid, R. Ullah, A. U. Rehman, M. Dildar, M. Ahmad, K. Ullah, M. N. Rafi, F. Teng. Porous Cu-based metal organic framework (Cu-MOF) for highly selective adsorption of organic pollutants, *Journal of Solid State Chemistry*, **2023**, *322*, 123935.
  23. X. Yang, J. Zhao, C. P. Artur, J. Su, H. Wang. Encapsulated laccase in bimetallic Cu/Zn ZIFs as stable and reusable biocatalyst for decolorization of dye wastewater, *International Journal of Biological Macromolecules*, **2023**, *233*, 123410.

24. M. Shahbakhsh, H. Saravani, M. Dusek, M. Poupon. Study of the one-step in situ growth synthesis of Cu-Pic coordination polymer and Cu-BTC MOF and their performances for detection of 4-Nitrophenol, *Microchemical Journal*, **2023**, 189, 108557.
25. Y. P. Yu, M. M. Pan, M. Jiang, X. Yu, L. Xu. Facile synthesis of self-assembled three-dimensional flower-like Cu-MOF and its pyrolytic derivative Cu-N-C450 for diverse applications, *Journal of Environmental Chemical Engineering*, **2023**, 11(2), 109400.
26. N. Faaizatunnisa, R. Ediati, H. Fansuri, H. Juwono, S. Suprpto, A. R. P. Hidayat, L. L. Zulfa. Facile green synthesis of core-shell magnetic MOF composites ( $\text{Fe}_3\text{O}_4@\text{SiO}_2@$ HKUST-1) for enhanced adsorption capacity of methylene blue, *Nano-Structures & Nano-Objects*, **2023**, 34, 100968.
27. N. Rabiee, M. Atarod, M. Tavakolizadeh, S. Asgari, M. Rezaei, O. Akhavan, A. Pourjavadi, M. Jouyandeh, E. C. Lima, A. H. Mashhadzadeh, A. Ehsani, S. Ahmadi, M. R. Saeb. Green metal-organic frameworks (MOFs) for biomedical applications, *Microporous and Mesoporous Materials*, **2022**, 335, 111670.
28. Y. Liu, P. Ghimire, M. Jaroniec. Copper benzene-1,3,5-tricarboxylate (Cu-BTC) metal-organic framework (MOF) and porous carbon composites as efficient carbon dioxide adsorbents, *Journal of Colloid and Interface Science*, **2019**, 535, 122-132.
29. D. Qian, C. Lei, G. P. Hao, W. C. Li, A. H. Lu. Synthesis of hierarchical porous carbon monoliths with incorporated metal-organic frameworks for enhancing volumetric based  $\text{CO}_2$  capture capability, *ACS Applied Materials & Interfaces*, **2012**, 4(11), 6125-6132.
30. R. Kaur, A. Kaur, A. Umar, W. A. Anderson, S. K. Kansal. Metal-organic framework (MOF) porous octahedral nanocrystals of Cu-BTC: synthesis, properties, and enhanced adsorption properties, *Materials Research Bulletin*, **2019**, 109, 124-133.
31. M. S. Hosseini, S. Zeinali, M. H. Sheikhi. Fabrication of capacitive sensor based on Cu-BTC (MOF-199) nanoporous film for detection of ethanol and methanol vapors, *Sensors and Actuators B: Chemical*, **2016**, 230, 9-16.
32. G. Latha, N. Devarajan, P. Suresh. Framework copper-catalyzed oxidative synthesis of quinazolinones: a benign approach using  $\text{Cu}_3(\text{BTC})_2$  MOF as an efficient and reusable catalyst, *ChemistrySelect*, **2020**, 5(32), 10041-10047.
33. C. Y. Chuah, T. H. Bae. Incorporation of  $\text{Cu}_3\text{BTC}_2$  nanocrystals to increase the permeability of polymeric membranes in  $\text{O}_2/\text{N}_2$  separation, *BMC Chemical Engineering*, **2019**, 1(1), 1-9.
34. J. R. Mason, J. N. Weyrich, H. Yang. Mechanistic study of porosity formation in liquid-assisted mechanochemical synthesis of metal-organic framework  $\text{Cu}_3(\text{BTC})_2$  for adsorption-based applications, *Sustainability*, **2022**, 14(15), 9150.
35. E. Irandoost, H. Farsi, A. Farrokhi. Effects of water content on electrochemical capacitive behavior of nanostructured  $\text{Cu}_3(\text{BTC})_2$  MOF prepared in aqueous solution, *Electrochimica Acta*, **2021**, 368, 137616.
36. X. T. Lu, Y. F. Pu, L. Li, N. Zhao, F. Wang, F. K. Xiao. Preparation of metal-organic frameworks  $\text{Cu}_3(\text{BTC})_2$  with amino-functionalization for  $\text{CO}_2$  adsorption, *Journal of Fuel Chemistry and Technology*, **2019**, 47(3), 338-343.
37. J. Xiao, Y. Zhang, T. C. Zhang, Y. Wang, S. Yuan.  $\text{Cu}_3\text{BTC}_2$  MOF-impregnated boron-doped biochar derived from orange peels for enhanced  $\text{NH}_3$  capture, *Applied Surface Science*, **2023**, 635, 157735.
38. B. H. Hameed, A. A. Ahmad. Batch adsorption of methylene blue from aqueous solution by garlic peel, an agricultural waste biomass, *Journal of Hazardous Materials*, **2009**, 164(2-3), 870-875.
39. M. C. Ncibi, B. Mahjoub, M. Seffen. Kinetic and equilibrium studies of methylene blue biosorption by *Posidonia oceanica* (L.) fibres, *Journal of Hazardous Materials*, **2007**, 139(2), 280-285.
40. W. Y. Siew, N. H. H. A. Bakar, M. A. Bakar, A. Z. Abidin. Influence of various Cu/Fe ratios on the surface properties of green synthesized Cu-Fe-BTC and its relation to methylene blue adsorption, *Journal of Hazardous Materials*, **2021**, 416, 125846.